(RESEARCH ARTICLE)

# Adaptive backstepping fractional-order nonsingular terminal sliding mode control of the continuous polymerization reactor

Danladi King Garba [1], Shuaibu Ochetengu Yakubu [1], Mukhtar Ibrahim Bello [2] and Muhammad Baballe Ahmad [3, *]

[1] Department of Mechanical Engineering, Nigerian Defence Academy, (NDA),Kaduna, Nigeria.
[2] Department of Computer Science, Kano State Polytechnic, Nigeria.
[3] Department of Mechatronics Engineering (NDA), Kaduna, Nigeria.

## Abstract

This paper proposes an adaptive backstepping fractional order nonsingular fast terminal sliding mode control (AB-FNTSMC) for a polymerization reactor subjected to model uncertainties and environmental disturbances. This controller ensures robust performance in both reaching and sliding mode phases. A fast terminal reaching law is employed to remove the chattering phenomena. An adaptation rules are used to update the upper bounds of the disturbances whose information are not required. A numerical simulation is deployed to evidence the superior performance of the AB-FNTSMC.

**Keywords:** Adaptive Control; Polymerization reactor; Fractional-order; Nonsingular Fast terminal sliding mode control

## 1. Introduction

In polymer chemistry, polymerization is a process in which the reacting monomers combined to form a high molecular compound [1], [2]. Polymerization reactions take place in chemical reactors (batch, semi-batch or continuous reactors [3]) at expeditious rate and may result in explosions if not sufficiently regulated. As such, it is crucial to control the operating conditions of the reactor. The operating conditions include but not limited to monomer concentration, reaction rate, reactor temperature, coolant flow rate, initiator type, [4], [5].

The contamination of measurements by sensor noises, purity of products, variation in feed conditions and degree of mixing make polymerization reactions difficult to be controlled directly or monitored accurately [6]. The Automatic Continuous Online Monitoring of Polymerization reactions (ACOMP), gives the real-time measurements of the process dynamic states [7], [8], [9], [10]. The limitation of ACOMP is that it hardly measured the complete state vector. Therefore, an observer is required to measure all the states [11].

An Extended Kalman Filter (EKF) is the most commonly used measurement method in chemical industries [12], [13]. In [14], an EKF has been used to measure the states of Methyl-Methacrylate (MMA) copolymerization. In [15], the melt index (MI) of propylene polymerization process has been estimated using least squares support vector machine. In [16], an EKF has been applied to measure the biogas composition in a Continuous Stirred Tank Reactor (CSTR). A hierarchical EKF has been used to estimate the kinetic parameters in the production of ethylene-propylenediene polymer [17].

* Corresponding author: Muhammad Baballe Ahmad

In order to compensate the uncertainties and external disturbances deteriorating the operations of chemical processes, sliding mode control (SMC) strategies are employed. In [18], an event driven SMC was proposed for a chemical reactor. A Sliding mode observer based control has been implemented in [19] for a fermentation process and in [20] for a batch polymerization reactor. In [21], a SMC was suggested for temperature control of a batch process. In [22], a decentralised SMC was developed for the control of two-input-two-ouyput chemical reactor. A temperature trajectory tracking SMC has been designed for a batch reactor [23].

The time-varying Parameters in chemical processes add more difficulties to the control design. An adaptive SMC based support vector machine was designed for a chemical reactor in [24]. In [25], a model free adaptive controller has been constructed to control molecular weight distribution in styrene polymerization. In [26], an adaptive control technique was implemented for a nonlinear wiener model and it was applied for composition control in a chemical reactor. Nonetheless, adaptive control schemes are limited to systems with constant or slow time varying parameters. This limitation can be lifted by deploying neural network (NN) to approximate the system dynamics. A NN based MPC was used for temperature control of a multi-product batch reactor [27]. A RBFNN based internal model controller was utilised to control the average molecular weight in the free radical polymerization of MMA. A NN based generic model control was developed for a multivariable semi-batch reactor [28]

Considering the foregoing discussion, in this paper, we integrate backstepping, fractional order nonsingular terminal sliding mode surface, and adaptive reaching laws to control the monomer concentration and the temperature of a polymerization reactor with uncertain dynamics. Furthermore, this is the first time a ABFNTSMC is proposed to control the reactor. The main contributions of this article include

In order to improve the robustness against disturbances, a FNTSM surface has been proposed. Moreover, by combining the FNTSMC with backstepping, the tracking accuracy is greatly enhanced.

In [18]-[23], the upper bounds of the disturbances are known. However, chemical processes have multiple operating points and therefore it is difficult to obtain the upper bounds of the dynamic disturbances at each operating region. As a result, we used adaptive laws to estimate the upper bounds of the disturbances. In addition, fast terminal reaching laws are utilised to do away with chattering effects.

A Lyapunov candidate function is used to show the convergence and the stability of the closed loop system.

The structure of the paper is arranged as follows: In Section 2 the dynamic model of the polymerization reactor is provided. In Section 3, the proposed control technique is developed. Simulation results and performance comparisons are provided in Section 4. Finally, we conclude our work in Section 5.

## 2. Mathematical Model

We consider the free radical polymerization of styrene monomers initiated by azobis-iso-butyronitrile dissolved in a pure benzene in a jacketed continuous stirred tank reactor depicted in Fig. 1. The heat released by the exothermic process is removed by a cooling jacket using water as the cooling fluid. The dynamic model of the reactor is derived from material and energy balance equations as [29]
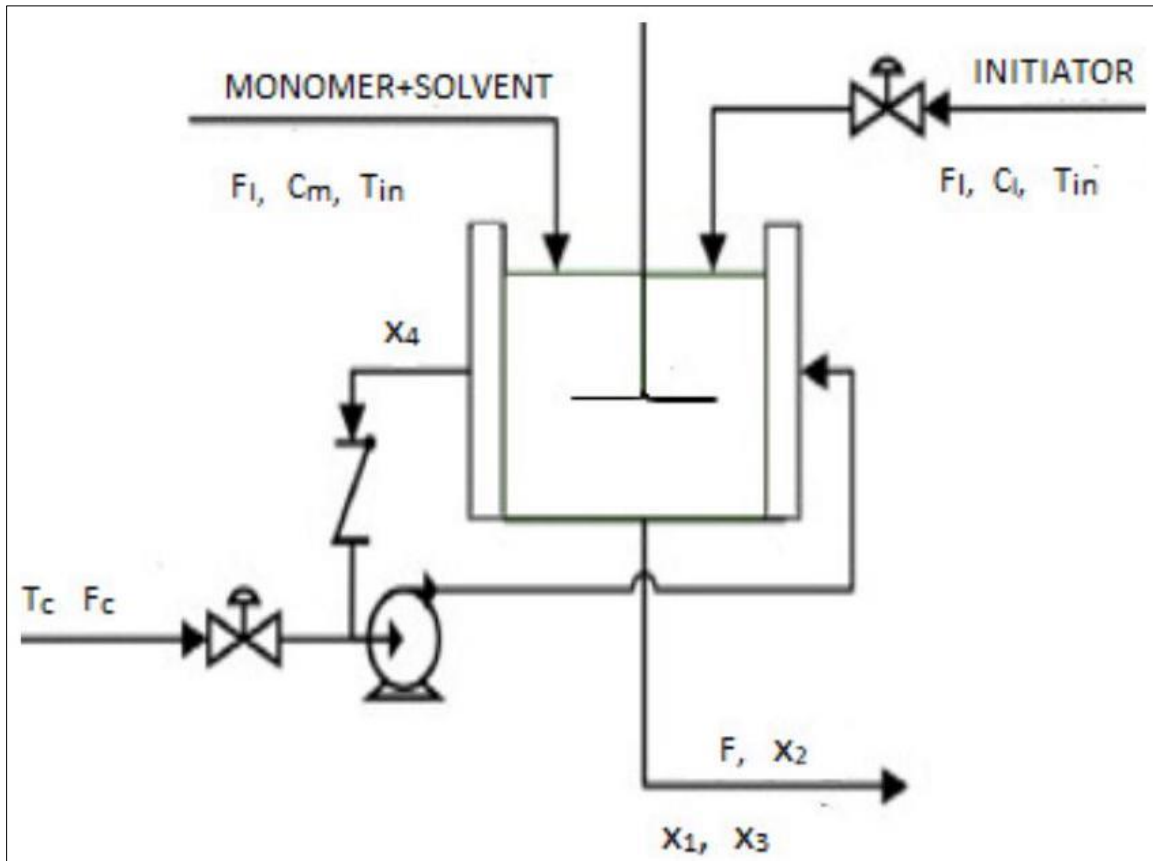
**Figure 1** A simple schematic diagram of the polymerization reactor

$$\dot{x}_1 = -\left(k_p + k_{fm}\right)\zeta_0 x_1 + \frac{F_m(C_m - x_1)}{v}. \tag{1}$$

$$\dot{x}_2 = -k_I x_2 + \frac{F_i C_I - F x_2}{v}. \tag{2}$$

$$\dot{x}_3 = k_p \frac{(-\Delta H_p)}{\rho c_p} x_1 \zeta_0 - \frac{UA}{\rho c_p v}(x_3 - x_4) + \frac{F(T_{in} - x_3)}{v}. \tag{3}$$

$$\dot{x}_4 = \frac{F_c T_c - F x_4}{v_c} + \frac{UA}{\rho_c c_c v_c}(x_3 - x_4). \tag{4}$$

$$\zeta_0 = \left[\frac{2fk_I}{k_{Tc} + k_{Td}}\right]^{1/2} \sqrt{x_2}.$$

$$M = x_1; \quad T = x_3. \tag{5}$$

where $x_1(\text{kmol/m}^3), x_2(\text{kmol/m}^3)$ denote the monomer and the initiator concentrations respectively, $x_3(^0K)$ and $x_4(^0K)$ stand for the reactor and the coolant's temperatures respectively. The outputs are $M = x_1$ and $T = x_3$. The inputs are the coolant flow rate $F_c\ m^3/h$ and the initiator flow rate $F_i m^3/h$. The definition and the values of the reactor parameters are given in Table 1.

## 2.1. Preliminaries

Definition 1 [30] The general definition of the fractionalorder derivative and integration is given by

$$_\theta \mathcal{D}_t^\mu = \begin{cases} \frac{d^\mu}{dt^\mu} & \text{Re}(\mu) > 0. \\ 1 & \text{Re}(\mu) = 0. \\ \int_\theta^t d\tau^\mu & \text{Re}(\mu) < 0. \end{cases} \tag{6}$$

where $\mathcal{D}$ is the fractional calculus operator, $\mu$ represents the fractional order which can be complex or real, $\theta$ and $t$ stand for the lower and upper limits of the

**Table 1** The definitions and values of the reactor parameters [29]

| Symbols | Values | Meaning |
|---|---|---|
| $v$ | $1.0m^3$ | Reactor volume |
| $T$ | $335K$ | Reactor temperature |
| $F$ | $10.0 m^3/h$ | Monomer flow rate |
| $f^*$ | 0.58 | Initiator efficiency |
| $k_p$ | $2.50 \times 10^6$ m$^3$/(kmol. h) | Propagation rate constant |
| $k_{Tc}$ | $1.33 \times 10^{10}$ m$^3$/(kmol. h) | Termination by coupling rate constant |
| $k_{Td}$ | $1.09 \times 10^{11}$ m$^3$/(kmol. h) | Termination by disproportionation rate constant |
| $C_m$ | 6.00kmol/m$^3$ | Inlet monomer concentration |
| $C_I$ | 8.00kmol/m$^3$ | Inlet monomer concentration |
| $K_I$ | $1.02 \times 10^{-1} h^{-1}$ | Initiation rate constant |
| $k_{fm\ rl}$ | $2.45 \times 10^3$ m$^3$/(kmol. h) | Chain transfer to monomer rate constant |
| $M_m$ | 100.12 kg/kmol | Molecular weight of the monomer |
| $\rho$ | 866kgm$^3$ | Density of the reacting mixture |
| $\rho_{c\ r} r_1$ | 1000 kg. m$^3$ | Density of water |
| $c_p$ | 2.0 kJ$_J$kg$^{-1} \cdot$ K$^{-1}$ | Heat capacity of the reacting mixture |
| $-\Delta H_p$ | 57800kJ. kmol$^{-1}$ | Heat of propagation reaction |
| $U$ | $720 kJ. h^{-1} \cdot K^{-1}$ | Overall heat transfer coefficient |
| $A$ | $2.0m^2$ | Heat transfer area |
| $c_c$ | $4.2 kj. $ kg$^{-1}. K^{-1}$ | Heat capacity of water |
| $T_{in}$ | $350K$ | Temperature of the inlet streams in the reactor |
| $T_c$ | $293.2K$ | Temperature of the inlet coolant stream |

operation, $\text{Re}(\mu)$ represents the real part $\mu$. The Riemann-Liouville definition of the fractional-order calculus is given by

$$_\theta \mathcal{D}_t^\mu = \left(\frac{d}{dt}\right)^n \frac{1}{\Gamma(n-\mu)} \int_\theta^t \frac{f(\tau)}{(t-\tau)^{\mu-n+1}}. \qquad (7)$$

$n-1 < \mu < n, n \in \mathcal{N}, \mu \in \mathcal{R}$ and $\Gamma(.) is a gamma$ function

Assumption 1 The disturbances are bounded $\Delta_i \le K_i (i = m, T)$

By differentiating $M$ and $T$ from (5) with respect to time, we have

$$\begin{cases} \dot{M} = \frac{\partial M}{\partial x_1} \dot{1} + \frac{\partial M}{\partial x_2} \dot{x}_2. \\ \dot{T} = \frac{\partial T}{\partial x_1} \dot{x}_1 + \frac{\partial T}{\partial x_2} \dot{x}_2 + \frac{\partial T}{\partial x_3} \dot{x}_3 + \frac{\partial T}{\partial x_4} \dot{x}_4. \end{cases} \qquad (8)$$

Differentiating (8) with respect to time yields

$$\begin{cases} \ddot{M} = \frac{\partial(\dot{M})}{\partial x_{1)}} \dot{x}_1 + \frac{\partial(\dot{M})}{\partial x_2} \dot{x}_2. \\ \ddot{T} = \frac{\partial(\dot{T})}{\partial x_1} \dot{x}_1 + \frac{\partial(\dot{T})}{\partial x_2} \dot{x}_2 + \frac{\partial(\dot{T})}{\partial x_3} \dot{x}_3 + \frac{\partial(\dot{T})}{\partial x_4} \dot{x}_4. \end{cases} \tag{9}$$

It is obvious that the inputs can be extracted from (9). Therefore

$$\begin{cases} \ddot{M} = A_1(x) + B_{11}(x)F_i. \\ \ddot{T} = A_2(x) + B_{21}(x)F_i + B_{22}(x)F_c. \end{cases} \tag{10}$$

where:

$$A_1(x) = \frac{\partial(\dot{M})}{\partial x_1} \dot{x}_1 + \frac{\partial(\dot{M})}{\partial x_2} \left[ -k_I x_2 + \frac{-F x_2}{v} \right]$$

$$A_2(x) = \frac{\partial(\dot{T})}{\partial x_1} \dot{x}_1 + \frac{\partial(\dot{T})}{\partial x_2} \left[ -k_I x_2 + \frac{-F x_2}{v} \right]$$

$$+ \frac{\partial(\dot{T})}{\partial x_3} \dot{x}_3 + \frac{\partial(\dot{T})}{\partial x_4} \left[ \frac{-F x_4}{v_c} + \frac{UA(x_3 - x_4)}{\rho_c c_c v_c} \right]$$

$$B_{11}(x) = \frac{C_I}{v} \frac{\partial(\dot{M})}{\partial x_2}, \ B_{21}(x) = \frac{\partial(\dot{T})}{\partial x_2} \frac{C_I}{v}$$

$$B_{22}(x) = \frac{\partial(\dot{T})}{\partial x_4} \frac{T_c}{v_c}, \ U_1 = F_i, \ U_2 = F_c$$

From (10), we have

$$\begin{cases} \dot{\xi}_1 & = \xi_2 \\ \dot{\xi}_2 & = A(x) + B(x)U + \Delta \end{cases} \tag{11}$$

where

$$\xi_1 = \begin{bmatrix} M_1 \\ T_1 \end{bmatrix}, \ \xi_2 = \begin{bmatrix} M_2 \\ T_2 \end{bmatrix}, \ A(x) = \begin{bmatrix} A_1(x) \\ A_2(x) \end{bmatrix},$$

$$U = \begin{bmatrix} U_1 \\ U_2 \end{bmatrix}, \ \Delta = \begin{bmatrix} \Delta_1 \\ \Delta_2 \end{bmatrix}, \ B(x) = \begin{bmatrix} B_{11}(x) & 0 \\ B_{21}(x) & B_{22}(x) \end{bmatrix}.$$

where $\Delta$ denotes the external disturbances. $B^{-1}(x)$ exists since $\det(B(x)) = B_1(x)B_2(x) \neq 0$.

## 3. Control design

In this section, the proposed AB-FNTSMC is dveloped for the control of monomer concentration and reactor temperature. In addition, a robust backstepping with integral sliding mode controller (RBISMC) and feedback linearization controller (FLC) are designed for comparison with the AB-FNTSMC.

### 3.1. Design of AB-FNTSMC

The tracking errors are expressed as

$z_1 = \xi_1 - \xi_d; \ \dot{z}_1 = \dot{\xi}_1 - \dot{\xi}_d = \xi_2 - \dot{\xi}_d.$

$z_2 = \xi_2 - \dot{\xi}_d; \ \dot{z}_2 = \dot{\xi}_2 - \ddot{\xi}_d$

where $z_1 = [z_m \quad z_T]^T, z_2 = [\dot{z}_m \quad \dot{z}_T]^T$ are the vectors of tracking errors and $\xi_d = [M_d \quad T_d]^T$ is the vector of the desired trajectories. The FNTSM surface is specified as [31]

$$S = z_2 + \Lambda_1 D^{\mu_1}[\text{sign}(z_1)^p] + \Lambda_2 D^{\mu_2 - 1}[\text{sign}(z_1)^q]. \tag{12}$$

where

$$S = \begin{bmatrix} S_M \\ S_T \end{bmatrix}; \; \Lambda_1 = \begin{bmatrix} \Lambda_{1m} & 0 \\ 0 & \Lambda_{1T} \end{bmatrix}; \; \Lambda_2 = \begin{bmatrix} \Lambda_{2m} & 0 \\ 0 & \Lambda_{2T} \end{bmatrix}$$

$$\text{sign}(z_1)^p = \begin{bmatrix} \text{sign}(z_m)^p \\ \text{sign}(z_T) \end{bmatrix} : \text{sign}(z_1)^q = \begin{bmatrix} \text{sign}(z_m)^q \\ \text{sign}(z_T)^q \end{bmatrix}.$$

The time derivative of the sliding surface (12) yields

$$
\begin{aligned}
\dot{S} &= \dot{z}_2 + \Lambda_1 D^{\mu+1}[\text{sign}(z_1)^p] + \Lambda_2 D^{\mu_2}[\text{sign}(z_1)^q] \\
&= \ddot{\xi}_2 - \ddot{\xi}_d + \Lambda_1 D^{\mu+1}[\text{sign}(z_1)^p] + \Lambda_2 D^{\mu_2}[\text{sign}(z_1)^q]. \\
&= A(x) + B(x)U + \Delta - \ddot{\xi}_d + \Lambda_1 D^{\mu+1}[\text{sign}(z_1)^p]
\end{aligned}
\tag{13}
$$

Select a Lyapunov function as

$$L_1 = \tfrac{1}{2} z_1^T z_1. \tag{14}$$

$$\dot{L}_1 = z_1^T \dot{z}_1 = z_1^T(\dot{\xi}_1 - \dot{\xi}_d) = z_1^T(\xi_2 - \dot{\xi}_d). \tag{15}$$

The virtual controller is designed as

$$\xi_2 = \dot{\xi}_d - C z_1 - S. \tag{16}$$

where $C = C^T > 0$ is a constant diagonal matrix. Inserting the virtual input (16) into (14) gives

$$\dot{L}_1 = -z_1^T C z_1 + z_1^T S \tag{17}$$

Consider the following Lyapunov function

$$L_2 = \tfrac{1}{2} z_1^T z_1 + \tfrac{1}{2} S^T S \tag{18}$$

Differentiating (18) with respect to time, we have

$$\dot{L}_2 = z_1^T \dot{z}_1 + S^T \dot{S} = -z_1^T C z_1 + S^T(z_1 + \dot{S}) \tag{19}$$

where

$$r = -\ddot{\xi}_d + \Lambda_1 D^{\mu+1}[\text{sign}(z_1)^p] + \Lambda_2 D^{\mu_2}[\text{sign}(z_1)^q]$$

To guarantee fast convergence and excellent tracking accuracy with the existence of model perturbations and disturbances, a FTSM reaching law is developed as

$$\dot{S} = -B(x)^{-1}[R_1 S + R_2 \text{sign}(S)^\vartheta]. \tag{20}$$

where $\text{sign}(S)^\vartheta = [\text{sign}(S_M)^\vartheta, \text{sign}(S_T)^\vartheta]^T$, $R_1$ and $R_2$ are unknown constant diagonal matrices. Therefore, the robust controller can be written as

$$U = B^{-1}(x)[-z_1 - A(x) - r - \hat{R}_1 S - \hat{R}_2 \text{sign}(S)^\vartheta]. \tag{21}$$

where $\hat{R}_i$ is the estimate matrices $\hat{R}_i (i = 1,2)$. The matrices are estimated by the following adaptation laws

$$
\begin{cases}
\dot{\hat{R}}_1 = \alpha_1 [\text{diag}(S)^T \text{diag}(S) - \kappa_1 \hat{R}_1]. \\
\dot{\hat{R}}_2 = \alpha_2 [\text{diag}(S)^T \text{diag}(\text{sign}(S))^\vartheta - \kappa_1 \hat{R}_2 \cdot]
\end{cases}
\tag{22}
$$

where $\alpha_1 = \alpha_1^T > 0, \alpha_2 = \alpha_2^T > 0$ are constant diagonal matrices, $\kappa_1 > 0, \kappa_2 > 0$ are small constants.

Theorem 1 For the input-output dynamics (11) under the FNFTSM surface (12), if the adaptive control law is established as (21) updated with (22), then, $S, z_1, z_2, \tilde{R}_1$, and $\tilde{R}_2$ are ultimately uniformly bounded.

Proof By augmenting the Lyapunov function (18), we get

$$L_2 = \frac{1}{2}z_1^T z_1 + \frac{1}{2}S^T S + \frac{1}{2}\tilde{R}_1^T \alpha_1^{-1}\tilde{R}_1 + \frac{1}{2}\tilde{R}_2^T \alpha_2^{-1}\tilde{R}_2. \tag{23}$$

Differentiating (23) with respect to time, we have

$$\begin{aligned}
\dot{L}_2 &= z_1^T \dot{z}_1 + S^T \dot{S} + \tilde{R}_1^T \alpha_1^{-1}\dot{\tilde{R}}_1 + \tilde{R}_2^T \alpha_2^{-1}\dot{\tilde{R}}_2 \\
&= -z_1^T C z_1 + S^T(z_1 + A(x) + B(x)U + \Delta + r)
\end{aligned} \tag{24}$$

Substituting the control input (21) into (24), one has

$$\dot{L}_2 = -z_1^T C z_1 + S^T\big(\Delta - \hat{R}_1 S - \hat{R}_2 \text{sign}(S)^\vartheta\big) \tag{25}$$

Noting that $\hat{R}_i = R_i - \tilde{R}_i (i = 1,2)$, we achieve

$$\begin{aligned}
\dot{L}_2 &= -z_1^T C z_1 + S^T\big(\Delta - R_1 S - R_2 \text{sign}(S)^\vartheta\big) \\
&\quad + \tilde{R}_1\Big[\text{diag}(S)^T\text{diag}(S) - \alpha_1^{-1}\dot{\hat{R}}_1\Big]
\end{aligned} \tag{26}$$

Substituting the update laws(22) into (26) yields

$$\dot{L}_2 = -z_1^T C z_1 - S^T R_1 S + S^T R_0 \text{sign}(S)^\vartheta \tag{27}$$

where $R_0 = \big[\text{diag}(\Delta)\text{diag}^{-1}\big(\text{sign}(S)^\vartheta\big) - R_2\big]$. Using the following Young's inequalities,

$$\tilde{R}_i \hat{R}_i = \tilde{R}_i[R_i - \tilde{R}_i] \leq \frac{\|R_i\|^2}{2} - \frac{\|\tilde{R}_i\|^2}{2}(i = 1,2)$$
$$S^T R_1 S \leq \| S \|^2 \|R_1\|; S^T R_0 \text{sign}(S)^\vartheta \leq \| S \|^{1+\vartheta} \|R_0\|;$$
$$\| S \|^{2(1+\vartheta)} \|R_0\|^2 \leq \| S \|^2 \|R_0\|^2, \| S \|^2 \to 0$$

Equation (27) can be written as

$$\dot{L} \leq -m\left[\frac{\|z_1\|^2}{2} + \frac{\| S \|^2}{2} + \frac{\|\tilde{R}_1\|^2}{2\|\alpha_1\|} + \frac{\|\tilde{R}_2\|^2}{2\|\alpha_2\|}\right]$$

$$+ \frac{\|R_1\|^2}{2} + \frac{\|R_2\|^2}{2} \tag{28}$$

Therefore,

$$L \leq -mL + n. \tag{29}$$

where $m = \min\{\| C \|, 2(\|R_1\| - \|R_3\|)\kappa\|\alpha_1\|, \kappa\|\alpha_2\|, n = \frac{\|R_1\|^2}{2} + \frac{\|R_2\|^2}{2}$. Integrating (38) yields

$$L \leq \frac{n}{m} + L(0)e^{-mt}. \tag{30}$$

As $t \to \infty, L \leq \frac{n}{m}$. Therefore, the closed loop signals are uniformly ultimately bounded in the compact set $\beta = \left\{L: L \leq \frac{n}{m}\right\}$

## 3.2. Design of RBISMC

The ISMC surface is defined as [32]

$$S = z_2 + \Pi_1 \int z_1 dt. \tag{31}$$

where $\Pi_1 = \Pi_1^T > 0$ is a constant diagonal matrices. The fictitious controller is designed as

$$\xi_2 = \dot{\xi}_d - C_2 z_1 - S. \tag{32}$$

where $C_2 = C_2^T > 0$ is a diagonal matrix. The control input is developed as

$$\begin{cases} U = U_{eq} + U_r. \\ U_{eq} = B^{-1}(x)[-A(x) + \ddot{\xi}_d - z_1 - \Pi_1 z_1]. \\ U_r = -B^{-1}(x)R_3 \text{sign}(S). \end{cases} \tag{33}$$

where $R_3 = R_3^T > 0$ is a diagonal matrix

**Theorem 2** For the input-output dynamics (10) controlled by (32) and (33) under the ISM surface (31), then the system is                                         asymptotically                                         stable.
Proof We consider the Lyapunov function

$$L_3 = \frac{1}{2} z_1^T z_1 + \frac{1}{2} S^T S. \tag{34}$$

By computing the time-derivative of (34), one gets

$$\dot{L}_3 = z_1^T \dot{z}_1 + S^T \dot{S} = z_1^T (\xi_2 - \dot{\xi}_d). \tag{35}$$

$$+ S^T (A(x) + B(x)U + \Delta - \ddot{\xi}_d + +\Pi_1 z_1).$$

Using the virtual controller (32), one has

$$\dot{L}_3 = -z_1^T C_2 z_1 + S^T [z_1 + A(x) + B(x)U + \Delta \tag{36}$$

From the control law (33), (36) becomes

$$\dot{L}_3 = -z_1^T C_2 z_1 + S^T [\Delta - R_3 \text{sign}(S)] \\ \leq -\|C_2\|\|z_1\|^2 - \| S \| [\|R_3 - \text{diag}(\Delta)\|]. \tag{37}$$

where $\tilde{R}_3 = R_3 - \text{diag}(\Delta) > 0$.

## 3.3. Design of FLC

Equation (10) can be rewritten as

$$\begin{bmatrix} \ddot{M} \\ \ddot{T} \end{bmatrix} = \begin{bmatrix} A_1(x) \\ A_2(x) \end{bmatrix} + \begin{bmatrix} B_{11}(x) & 0 \\ B_{21}(x) & B_{22}(x) \end{bmatrix} \begin{bmatrix} U_1 \\ U_2 \end{bmatrix}. \tag{38}$$

The global feedback linearization input is thus

$$U = \begin{bmatrix} U_1 \\ U_2 \end{bmatrix} = -\begin{bmatrix} B_{11}(x) & 0 \\ B_{21}(x) & B_{22}(x) \end{bmatrix}^{-1} \begin{bmatrix} A_1(x) \\ A_2(x) \end{bmatrix} + \begin{bmatrix} \Omega_1 \\ \Omega_2 \end{bmatrix}. \tag{39}$$

where $\Omega_i (i = 1,2)$ are auxiliary inputs. If $A_i(x), B_i(x)$ $(i = 1,2)$ are completely available, using (39), (38) becomes

$$\begin{cases} \ddot{M} = \Omega_1. \\ \ddot{T} = \Omega_2. \end{cases} \tag{40}$$

Then, the linearized system is thus

$$\begin{bmatrix} \dot{M_1} \\ \dot{M_2} \\ \dot{T_1} \\ \dot{T_2} \end{bmatrix} = \begin{bmatrix} 0 & 1 & 0 & 0 \\ 0 & 0 & 0 & 0 \\ 0 & 0 & 0 & 1 \\ 0 & 0 & 0 & 0 \end{bmatrix} \begin{bmatrix} M_1 \\ M_2 \\ T_1 \\ T_2 \end{bmatrix} + \begin{bmatrix} 0 & 0 \\ 1 & 0 \\ 0 & 0 \\ 0 & 1 \end{bmatrix} \begin{bmatrix} \Omega_1 \\ \Omega_2 \end{bmatrix}. \tag{41}$$

Therefore, the auxiliary controller is chosen as

$$\begin{cases} \Omega_1 = \ddot{M}_d + R_{pM} z_M + R_{iM} \int z_M dt + R_{dM} \frac{dz_M}{dt}. \\ \Omega_2 = \ddot{T}_d + R_{pT} z_T + R_{iT} \int z_T dt + R_{dT} \frac{dz_T}{dt}. \end{cases} \tag{42}$$

where $R_{pj}, R_{ij}$, and $R_{dj} (j = M, T)$ are the proportional, integral and derivative gains.

**Table 2** The control parameters

| Controllers | Values |
|---|---|
| AB-FNTSMC | $\Lambda_1 = \text{diag}(2.4, 3.7), \Lambda_2 = \text{diag}(1.1, 2.6)$ |
| | $\mu_1 = \mu_2 = 0.9, p = 0.5, q = 1.5$ |
| | $C = \text{diag}(13, 22)$ |
| | $\alpha_1 = \text{diag}(0.05, 0.01), \alpha_2 = \text{diag}(0.9, 4)$ |
| RBISMC | $\Pi_1 = \text{diag}(18, 30), C_2 = \text{diag}(8, 15)$ |
| | $R_3 = \text{diag}(12, 16)$ |
| FLC | $R_{pM} = 21, R_{dM} = 13, R_{iM} = 3$ |
| | $R_{pT} = 14, R_{dT} = 9, R_{iT} = 1.6$ |

## 4. Simulation results

In this section, simulation results are provided to show the satisfactory performance of the AB-FNTSMC designed. In addition, the Proposed AB-FNTSMC is compared with RBISMC and FLC. The parameters of the reactor are given in Table 1. The states of the process are simulated with an initial value of $x_i(0) = 0.001$ ( i = 1,2,3,4 ). A model uncertainty of 30% and external disturbances $\Delta_1 = 2, \Delta_2 = 18$ have been considered in the simulation. The parameters of the controllers are provided in Table 2.

The simulation results for the polymerization reactor control are presented in Figs. 2-6. As shown in Fig. 2, the FLC failed to trace the reference trajectories in the presence of dynamic uncertainties. Due to the robustness of the RBISMC, it is able compensate the uncertainties and track the reference signals. The responses of the outputs under the AB-FNTSMC are superior compared to both FLC and RBISMC due to its adaptive nature and robustness of the FNTSM surface. The tracking errors depicted in Fig. 3 converge to zero at a quicker rate under the AB-FNTSMC. The control signals of the AB-FNTSMC have no chattering unlike the RBISMC as shown in 4. The evolution of the parameters of reaching laws are shown in Fig. 5 and Fig. 6.
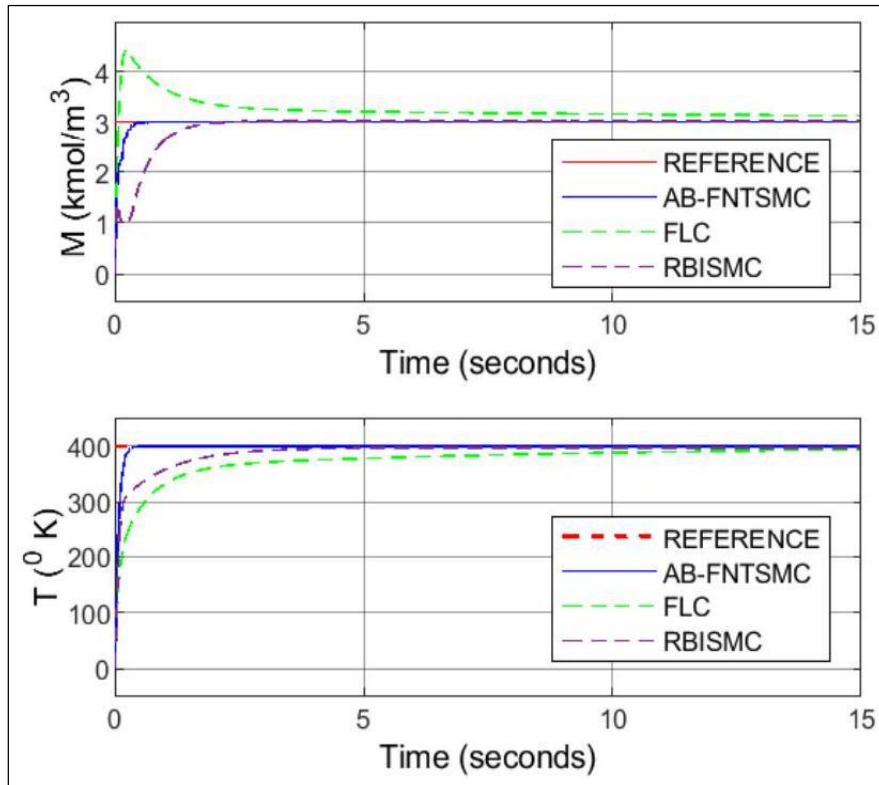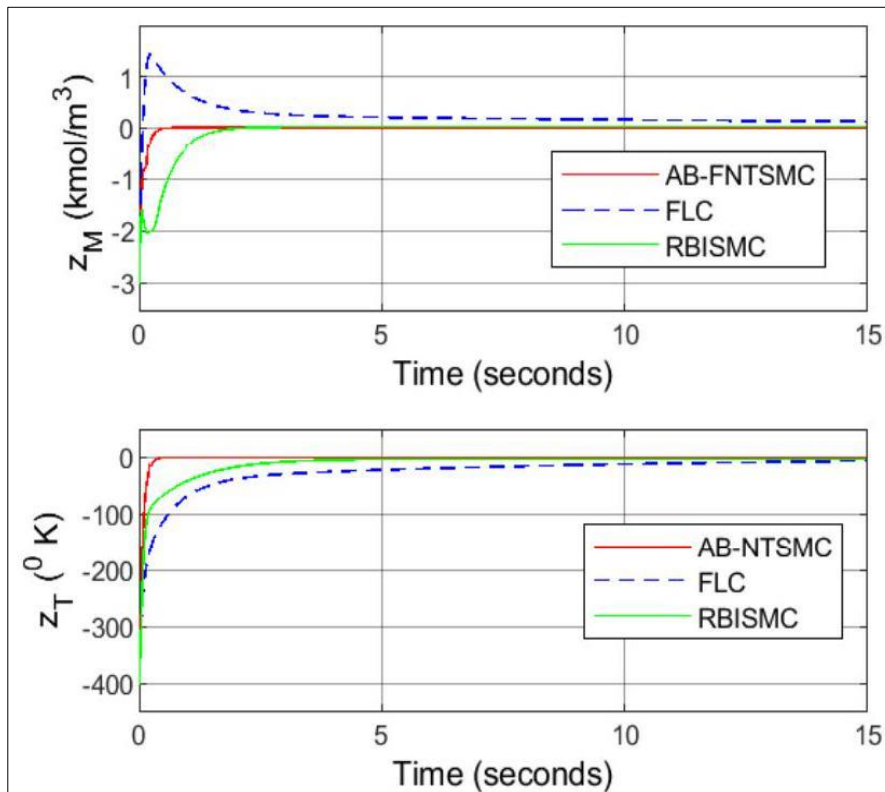
**Figure 2** Outputs' tracking
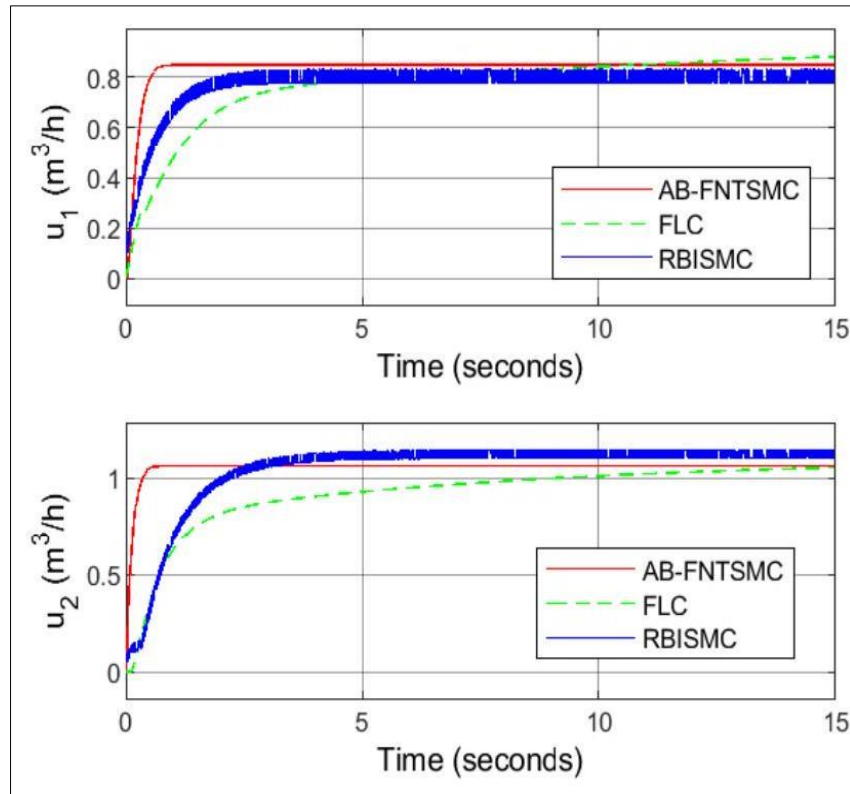


**Figure 3** Position tracking result

**Figure 4** The control inputs
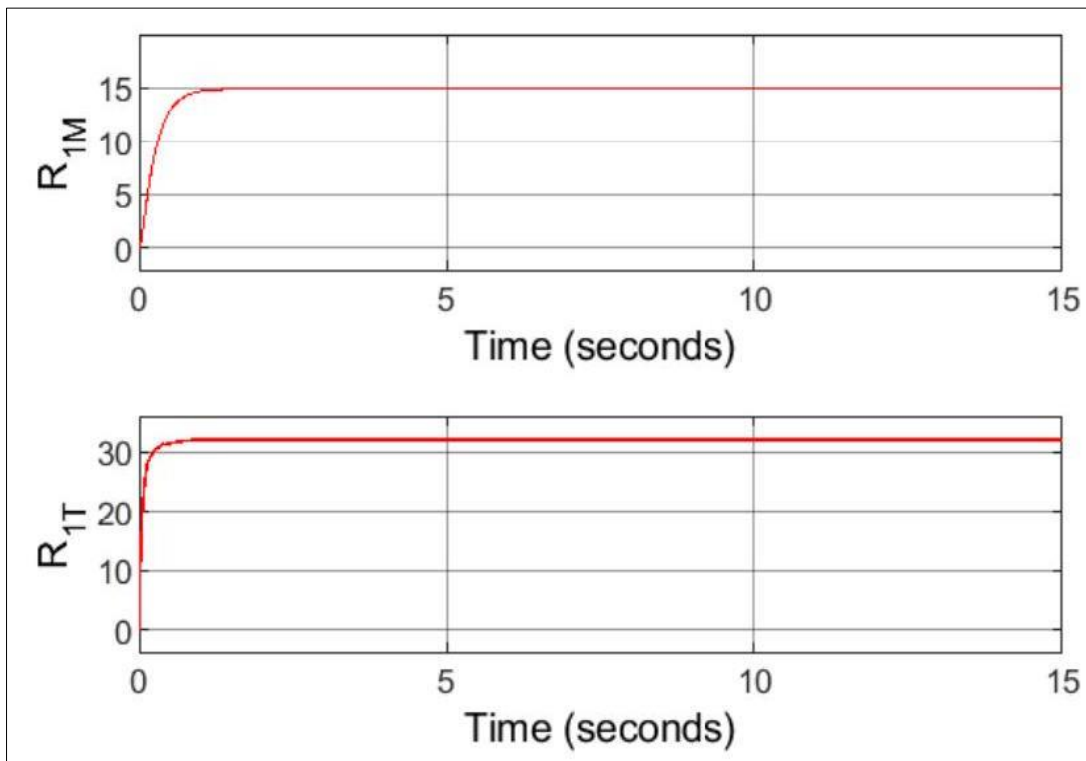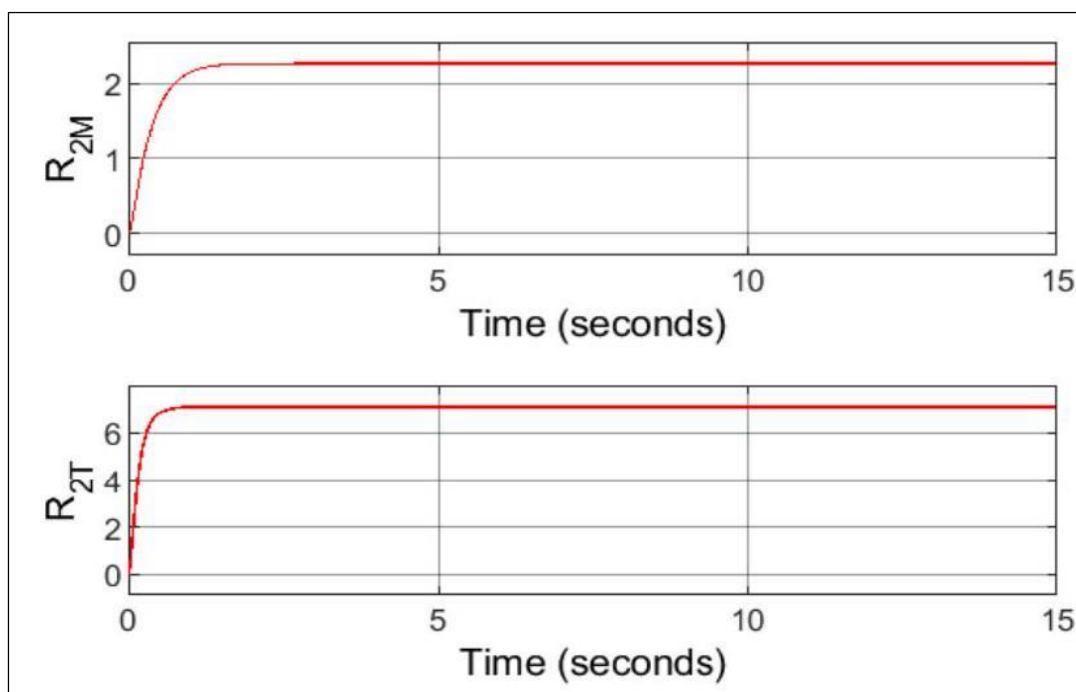


**Figure 5** Elements of the matrix $R_1$

**Figure 6** Elements of the matrix $R_2$

## 5. Conclusions

A robust AB-FNTSMC scheme for an uncertain polymerization reactor is developed in this article. The proposed controller admits strong robustness against external disturbances and uncertain model parameters. The chattering phenomena have been eliminated with the aid of fast terminal reaching laws with adaptive gains. Finally, some simulations have been executed to illustrate the efficiency of the devised method compared to FLC and RBISMC.

## Compliance with ethical standards

*Disclosure of conflict of interest*

No conflict of interest to be disclosed.

## References

[1] H. R. Allcock, F. W. Lampe, J. E. Mark, Contemporary polymer chemistry (3rd edition), Pearson Education, Inc (Pearson/Prentice Hall), Upper Saddle River, NJ, USA, 2003.

[2] C. Jonathan, N. Greeves, S. G. Warren, Organic chemistry Oxford University Press, Oxford, 2002.

[3] O. Levenspiel (2002) The Chemical Reactor Omnibook, Oregon St Univ Bookstores, Upper Saddle River, NJ, USA.

[4] J. R. Richards, J. P. Congalidis, "Measurement and control of polymerization reactors", Computers and Chemical Engineering, vol. 30, pp. 1447-1463, 2006.

[5] J. Kong, X. Chen, "Dynamic optimization of batch free radical polymerization with conditional modeling formulation through the adaptive smoothing strategy", Computers & Chemical Engineering, vol.120, pp. 15-29, 2019.

[6] L. W. McKeen, 10-high temperature polymers, in: L. W. McKeen (Ed.), Effect of Temperature and other Factors on Plastics and Elastomers (Second Edition), Plastics Design Library, William Andrew Publishing, Norwich, NY, pp. 503-550, 2008 .

[7] Tomasz Kreft, Wayne F. Reed, "Predictive control and verification of conversion kinetics and polymer molecular weight in semi-batch free radical homopolymer reactions", European Polymer Journal, Vol. 45, no. 8, Pp. 2288-2303, 2009.

[8]     T. Kreft, W. F. Reed, "Predictive control of average composition and molecular weight distributions in semi-batch free radical copolymerization reactions", Macromolecules, vol. 42, no. 15, pp. 5558-5565, 2009.

[9]     T. McAfee, et al., "Automatic control of polymer molecular weight during synthesis", Macromolecules, vol. 49, no. 19 , pp. 7170-7183, 2016.

[10]    F. H. Florenzano, R. Strelitzki, W. F. Reed, "Absolute, on-line monitoring of molar mass during polymerization reactions", Macromolecules, vol. 31, no. 21, pp. 7226-7238, 1998.

[11]    Giuseppe Leu, Roberto Baratti, "An extended Kalman filtering approach with a criterion to set its tuning parameters; application to a catalytic reactor", Computers & Chemical Engineering, Vol. 23, pp. 1839-1849, 2000.

[12]    S. Salas, et al. "Framework design for weight-average molecular weight control in semi-batch polymerization", Control Engineering Practice, vol. 78, pp. 12-23, 2018.

[13]    D. Dochain, A. Pauss, "On-line estimation of microbial specific growth-rates: An illustrative case study", The Canadian Journal of Chemical Engineering, vol. 66, no. 4, pp. $626 - 631$,1998.

[14]    M.-J. Park, S.-M. Hur, H.-K. Rhee, "Online estimation and control of polymer quality in a copolymerization reactor", AIChE Journal, vol. 48 no. 5 pp. 1013-1021, 2002.

[15]    Z. Cheng, X. Liu, "Optimal online soft sensor for product quality monitoring in propylene polymerization process", Neurocomputing, vol. 149, pp. 1216-1224, 2015.

[16]    M. J. Kupilik, T. L. Vincent, "Estimation of biogas composition in a catalytic reactor via an extended kalman filter", in: 2011 IEEE International Conference on Control Applications (CCA), pp. 768-773, 2011.

[17]    R. Li, A. B. Corripio, M. A. Henson, M. J. Kurtz, "Online state and parameter estimation of epdm polymerization reactors using a hierarchical extended kalman filter", Journal of Process Control, vol. 14, no. 8, pp. 837 -852, 2004.

[18]    A. Sinha, R. K. Mishra, "Control of a nonlinear continuous stirred tank reactor via event triggered sliding modes", Chemical Engineering Science, vol. 187, pp. 52-59, 2018.

[19]    R. Aguilar-López, R. Maya-Yescas, "State estimation for nonlinear systems under model uncertainties: a classof sliding-mode observers", Journal of Process Control, vol. 15, no.3, pp. 363-370, 2005.

[20]    A. F. Rahman, S. K. Spurgeon, X. G. Yan, "Sliding mode observer based control for a continuous fermentation process", in: IET Seminar Digest, pp. 854-859, 2010.

[21]    K. Narwekar, V. A. Shah (2020) Temperature control using sliding mode control: An experimental approach, in: M. Tuba, S. Akashe, A. Joshi (Eds.), Information and Communication Technology for Sustainable Development, Springer Singapore, Singapore, pp. 531-538.

[22]    C. B. Kadu, A. A. Khandekar, C. Y. Patil, "Sliding mode controller with state observer for tito systems with time delay", International Journal of Dynamics and Control, vol. 6 , no. 2 pp. 799-808, 2018.

[23]    C.-T. Chen,"A sliding mode control strategy for temperature trajectory tracking in batch processes", IFAC Proceedings, 8th IFAC Symposium on Advanced Control of Chemical Processes, vol. 45, no.15, pp. 644-649, 2012.

[24]    K. Uçak, G. Öke Günel, "An adaptive sliding mode controller based on online support vector regression for nonlinear systems", Soft Computing, pp. 1-21, 2019.

[25]    H. Wu, Y. Chen and J. Wang (2017) "Model-free output feedback control of molecular weight distribution," 2017 6th Data Driven Control and Learning Systems (DDCLS), Chongqing, pp. 473-478.

[26]    Ping Yuan, Bi Zhang, Zhizhong Mao (2017) A self-tuning control method for Wiener nonlinear systems and its application to process control problems, Chinese Journal of Chemical Engineering, Volume 25, Issue 2, Pages 193-201.

[27]    R. Kamesh and K. Y., Rani (2017) "Novel Formulation of Adaptive MPC as EKF Using ANN Model: Multiproduct Semibatch Polymerization Reactor Case Study," in IEEE Transactions on Neural Networks and Learning Systems, vol. 28, no. 12, pp. 3061-3073.

[28]    Kamesh, R., and Rani, K. Y., "Application of artificial neural network-based generic model control to multivariable processes", Asia-Pac. J. Chem. Eng.,vol. 12, pp. 775789,2017.

[29]    P. Biswas and A. N. Samanta, "Backstepping control of polymerization reactor," 2013 9th Asian Control Conference (ASCC), Istanbul, pp. 1-5, 2013.

[30] S. Chen, H. Chiang, T. Liu and C. Chang, "Precision Motion Control of Permanent Magnet Linear Synchronous Motors Using Adaptive Fuzzy Fractional-Order Sliding-Mode Control," in IEEE/ASME Transactions on Mechatronics, vol. 24, no. 2, pp. 741-752, 2019.

[31] Yaoyao Wang, et al., "Adaptive super-twisting fractionalorder nonsingular terminal sliding mode control of cabledriven manipulators", ISA Transactions, vol. 86, pp. 163180,2019.

[32] Ullah, S., Mehmood, A., Khan, Q. et al. "Robust Integral Sliding Mode Control Design for Stability Enhancement of Under-actuated Quadcopter", Int. J. Control Autom. Syst., vol. 18 , pp. $1671 - 1678, 2020$.